

A configurable electronics system for the ESS-Bilbao Beam Position Monitors

L. Muguira^{a,*}, D. Belver^a, V. Etxebarria^b, S. Varnasseri^a, I. Arredondo^a, M. del Campo^a, P. Echevarria^a, N. Garmendia^a, J. Feuchtwanger^a, J. Jugo^b, J. Portilla^b

^aESS-Bilbao, Edificio Rectorado, Vivero de Empresas, 48940, Leioa (Bizkaia), Spain.

^bUniversity of Basque Country (UPV/EHU), Dep. of Electricity and Electronics, Science and Technology Faculty, 48940, Leioa (Bizkaia), Spain.

Abstract

A versatile and configurable system has been developed in order to monitorize the beam position and to meet all the requirements of the future ESS-Bilbao Linac. At the same time the design has been conceived to be open and configurable so that it could eventually be used in different kind of accelerators, independently of the charged particle, with minimal change. The design of the Beam Position Monitors (BPMs) system includes a test bench both for button-type pick-ups (PU) and striplines (SL), the electronic units and the control system. The electronic units consist of two main parts. The first part is an Analog Front-End (AFE) unit where the RF signals are filtered, conditioned and converted to base-band. The second part is a Digital Front-End (DFE) unit which is based on an FPGA board where the base-band signals are sampled in order to calculate the beam position, the amplitude and the phase. To manage the system a Multipurpose Controller (MC) developed at ESSB has been used. It includes the FPGA management, the EPICS integration and Archiver Instances. A description of the system and a comparison between the performance of both PU and SL BPM designs measured with this electronics system is fully described and discussed.

Keywords:

Beam Position Monitor
Electronic Units
Control System
Sensitivity
Resolution

1. Introduction

Beam position monitors (BPMs) are the most frequently used non-interceptive diagnostic in particle accelerators, since they provide essential information both for precise monitoring and control of the beamline, and in general for the operation and optimization of the machine.

The term “beam position” refers to the center of gravity within the intensity distributions in the two coordinates transverse to the beamline [1], but also much more information such as tune, chromaticity, current, bunch shape or energy measured via time-of-flight can, in principle, be extracted from beam position measurements. For all these reasons, BPMs and, in particular, the corresponding driving electronics systems, remain a very active field of research in accelerator science and technology.

There are several ways of non-interceptively determining the position of the beam [2]. The most common method is based on capacitive coupling to the electromagnetic fields. To get the position of the beam, the signals from the electrodes of a beam monitor have to be compared. Determining the beam position from the ratio of the induced charges of the opposite electrodes could have different solutions depending on the type of

particle accelerator. The various signal processing systems can be grouped into different families according to the employed techniques as can be found for instance in Shafer [2] and Vismara [3]. Key factors in this context are, among others, signal acquisition, normalization, and recombination. Some possible techniques available for the normalization process of the BPM sensor signals are the logarithmic conversion, the amplitude to time and the amplitude to phase normalization. For the signal recombination, individual signal treatment and the $\frac{\Delta}{\Sigma}$ algorithm are common techniques. Finally, the acquisition can be carried out in wide-band, narrow-band and using slow acquisition.

Analog electronics is required to conditioning the signal from the electrodes to the properties of the analog to digital converters (ADCs) and an appropriate trigger must be used for the digitalization. The acquisition system fulfills the requirements needed to supply a full set of data from the BPM to the digital processor. Some implementations of different types of commercial electronics acquisition systems can be found in the literature. In Suwada et al. [4], a data-acquisition system based on VME/OS-9 computers has been developed in order to control 90 stripline BPMs in real time for the KEKB injector linac. All analog signals are connected with monitor stations. In Cohen-Solal [5], the voltage signals coming from four capacitive coupling detectors for the proton IPHI linac were processed by a commercial log-ratio BPM electronics module from Bergoz [6]

*Corresponding author. Tel.:(+34) 94 601 8198.

Email address: lmuguira@essbilbao.org (L. Muguira)

48 and an acquisition system based on National Instruments PXI.
 49 One of the solutions most commonly used for BPMs nowadays
 50 is the commercial solution offered by Libera [7], as can be seen
 51 for example, in Hartmann et al. [8].

52 Furthermore, different proprietary solutions have been also
 53 implemented. In this context, in Los Alamos National Labora-
 54 tory, different log-ratio techniques have been developed for
 55 BPM systems, similar to the ESS-Bilbao (ESSB) solution. In
 56 Wells et al. [9] they developed a log-ratio circuit using a logar-
 57 ithmic response circuit for a pair of microstrip probe sensors to
 58 obtain the beam position. In Shurter et al. [10] a different log-
 59 arithmic amplifier board has also been selected because its dy-
 60 namic range and bandwidth makes an excellent beam signal dete-
 61 ctor as compared to other techniques. The signals were digit-
 62 ized by a 14-bit ADC. In the experiment described in Walston
 63 et al. [11] they tried to understand the limits of the BPM per-
 64 formance and evaluate their applicability to issues posed by the
 65 ILC. An estimation that an RF cavity BPM could provide a po-
 66 sition measurement resolution of less than 1 nm was done. The
 67 resolution was measured using an in-house analog and digital
 68 electronics with fitting and digital down-conversion (DDC) al-
 69 gorithms with nine regression coefficients.

70 The systems mentioned above are not tailored to ESSB re-
 71 quirements, neither in terms of accuracy or stability specifica-
 72 tions, nor in terms of getting an all-in-one serializable solution,
 73 ready to be connected to an EPICS control environment. Thus
 74 the main motivation of this work has been to develop an inte-
 75 grated solution fulfilling the requirements, being at the same
 76 time a versatile, open and configurable deployment, potentially
 77 adaptable to other accelerators.

78 Considering the ubiquitous nature of BPMs in any kind of
 79 charged particle accelerators, the aim of this work is to present
 80 a new electronics system for the BPMs of ESSB, but conceived
 81 to be open and configurable so that it could eventually be used
 82 in different kind of accelerators, independently of the charged
 83 particle, with minimal change. This work has been developed
 84 in collaboration between the ESSB [12] and the Department
 85 of Electricity and Electronics of the University of the Basque
 86 Country (UPV/EHU) to fulfill the requirements of the ESSB
 87 accelerator facilities (see Table 1).

88 The developed BPM electronics system is composed of the
 89 analog front-end electronic boards, the digital processing board
 90 and the corresponding control system. Two types of BPM dete-
 91 ctors, capacitive buttons pick-ups (PU) and striplines (SL),
 92 have been designed and tested to verify the electronics system.
 93 The presented BPM system has been tested using an in-house
 94 test bench to simulate the beam displacement in typical proton
 95 or deuteron beamlines, with working frequencies 352 MHz and
 96 175 MHz respectively, thus checking its versatility. The system
 97 works as expected, in a wide variety of situations, for proton or
 98 ions frequencies and button-type or stripline electrode config-
 99 urations.

100 The contents of this article is divided in different parts. First
 101 of all, the ESSB BPM system is described. Next a section ex-
 102 plains the electronics units and the control system. Then the
 103 calibration and the sensitivity of the proposed BPM system is
 104 presented. Finally, a last section explaining the different tests

Table 1: Main ESSB and BPM parameters

Parameter	Value	Unit
Beam Parameters		
Maximum beam energy	60	MeV
Maximum current	75	mA
Maximum pulse length	1.8	ms
Maximum repetition rate	50	Hz
Resolution and precision requirements		
Position resolution	10	μm
Position stability	100	μm
Phase resolution	0.3	$^\circ$
Phase stability	2	$^\circ$
Signal levels at the electronics input		
Input power range	50	dB
Maximum input power	-10	dBm
Minimum input power	-60	dBm

developed to validate the proposed design is also included.

2. ESS-Bilbao BPM system

Table 1 summarises the parameters used in the design of the BPM electronics. It describes the main parameters of the beam, the signal levels at the entrance of the BPM electronics and the resolution and stability requirements.

The ESSB requirements for the BPMs are quite stringent for a proton linac, aiming at a position stability below $100 \mu\text{m}$, a position resolution below $10 \mu\text{m}$, a phase stability below 2° and a phase resolution below 0.3° .

The experimental setup consists of four different parts (Fig. 1) that will be described in the next sections [13]:

- The BPM Test Stand.
- The Analog Front-End (AFE) unit.
- The Digital Front-End (DFE) unit.
- The Control System.

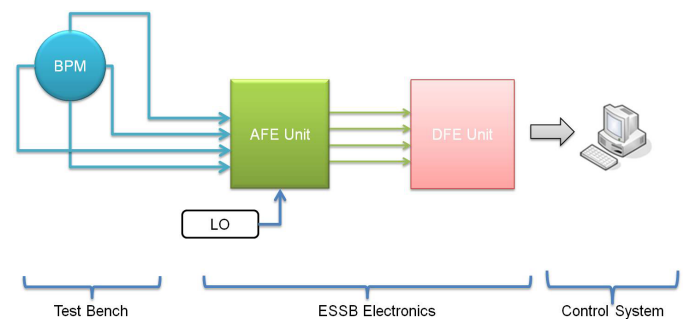


Figure 1: Simplified diagram of the BPM system.

2.1. BPM Test Stand

The test stand for simulating beam conditions was designed and fabricated at ESSB and UPV/EHU. The test bench is connected to the AFE unit as well as to the necessary RF equipment to simulate the beam. This implementation allows to test the developed electronics with the prototype BPM system.

The test bench is basically a transmission line composed of an internal static tube and a second movable outer tube [13]. The relative position of the internal one can be changed to simulate the beam displacement within a range of 20 mm for both axis with a position resolution of less than 10 μm using the corresponding micrometer knobs. A RF generator is connected to the transmission line to simulate the beam. In this study, the main frequencies of interest have been 175 MHz and 352 MHz.

Two types of beam position monitor detectors have been designed and implemented, SL and button-type PU. These detectors are commonly used as the front transducers for beam position monitoring in particle accelerators. They allow to detect the transverse position of the beam in the chamber with a $\frac{\Delta}{\Sigma}$ algorithm [2]. Using the same test bench and test mechanisms, both kind of electrode configurations have been tested. The assembling conditions of both kind of detectors have been kept as similar as possible to make an accurate comparison between them.

2.2. Pick-up configuration

This BPM design is based on four metalized ceramic feedthroughs as button PU welded to the beam pipe. These four ceramic feedthroughs are standard buttons from the industry [14], manufactured using metalized brazed ceramic and modelled for an impedance matching of 50 Ω , avoiding the resonance in the interest frequency range. This is reached varying the diameter and the thickness of the ceramic disc. The diameter of the center conductor is 1 mm, being the button diameter 12.2 mm. The feedthrough assembly angles have been fixed in 0, $\pi/2$, π and $3\pi/2$ configuration, as shown in Fig. 2.

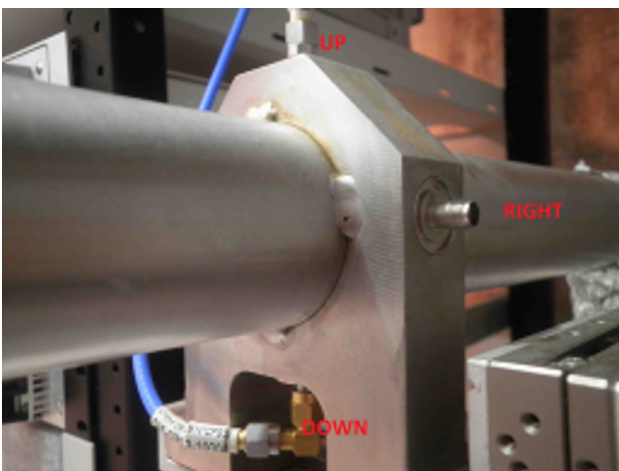


Figure 2: ESSB BPM test bench with PU, showing the position of the detectors.

2.3. Stripline configuration

The design of the SL detectors [15] is based on travelling wave sensors principles. In general, this type of detectors have well defined behaviour even for low beta and low intensity beams, as well as good functionality at low and high frequencies. SUPERFISH (2D) code has been used to simulate the physical properties and dimensions of the feedthrough and transition from strips to the outside N-type connector, as well as to find the optimum physical dimensions of the strips along the tube by analyzing the electromagnetic behaviour of the whole SL set.

The length of sensors is 200 mm and the tube chamber inner diameter of the SL set is 57 mm. The response of all detectors are identical ideally and they are located with a rotation of $\pi/4$ in the transverse plane of the tube (Fig. 3). The assembly angles of the strip sensors are $\pi/4$, $3\pi/4$, $5\pi/4$ and $7\pi/4$. Each electrode has a coverage angle of 0.952 rad. If this area were increased, coupling between adjacent sensors could happen, deteriorating the signal integrity.

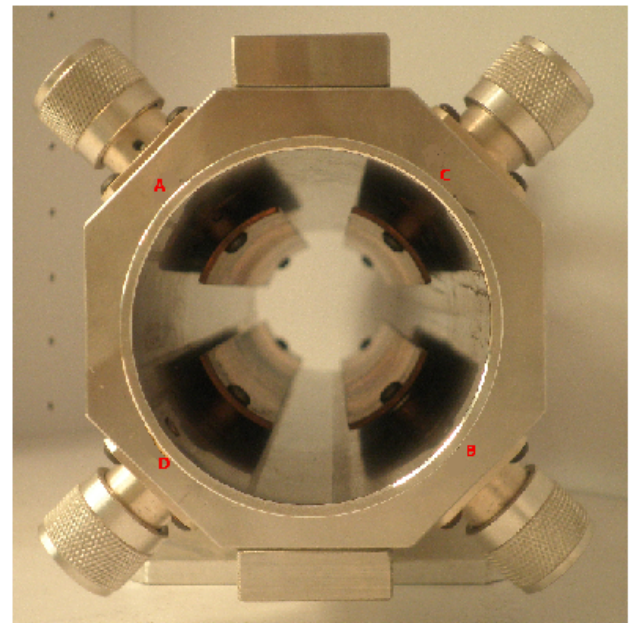


Figure 3: Internal view of the assembled SL in the laboratory, showing the position of the 4 detectors.

2.4. Comparison between both BPM configurations

As was explained above, the assembly of the test-bench is particular for each type of detector. In the PU case, the detectors are located over the X and Y axis, nevertheless, in the SL case, they are rotated at 45° from the axis. Moreover, the PUs are easy to install due to its small size in comparison with the SL.

Analyzing the measurement results, the PU detectors present a smoother power response in a broader frequency band, but their measured signal level is weaker, which can make this solution to be inappropriate for low beam currents and for low frequencies. On the other hand, SL detectors can provide more accurate positioning for low beam currents because they present higher output voltage. Furthermore, they could be used for very

low frequencies but the detector size can be a problem for fabrication and installation.

Fig. 4 depicts the measured signal power with both detectors in the test-bench in a frequency range from low-frequency to 1.5 GHz and for an input signal power of 0 dBm. A smoother response of PU detectors can be observed while SL detectors exhibit a typical periodic behavior [2]. It can also be noted the higher sensitivity of SL detectors and specially at low frequencies, below 100 MHz, where the signal level of the PU is very small.

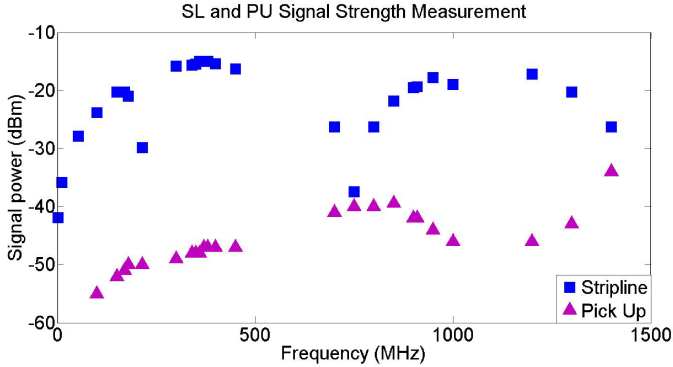


Figure 4: PU and SL power measurements up to 1.5 GHz.

In addition, the signal magnitude measured by the sensors was studied for a simulated beam of 352 MHz, and found to vary linearly with the input signal power in the range from -15 dBm to 20 dBm. In the SL case, the measured signal varies from -30 dBm to 0 dBm, whereas in the PU case, it varies from -60 dBm to -25 dBm. For an input signal of 0 dBm, the SL electrode detected -15 dBm and the PU electrode detected -44 dBm.

Regarding the detected voltage variation to displacement, the fitting equations for calculating the electrode voltage related to the applied displacement for each axis were calculated. PU sensors had more similar slope values than SL for both axes due to their accuracy in the fabrication procedure. Anyway the presented values are smaller because the sensitivity of the PUs is smaller.

The isolation between adjacent detectors was characterized using a vector network analyzer. Results in Fig. 5 show that isolation is much better for PU. It can be observed that, in this case, the coupling between detectors is so low that experimental results are close to the noise floor of the measurement system. Vector network analyzer measurements also confirm that the characteristic impedance of the SL detectors was around 50 Ω as desired, and PU detectors present a capacitive behaviour around 352 MHz.

3. Electronic Units and BPM control system

The Electronic Units could be divided in two parts: the AFE and the DFE units.

- An AFE unit where the RF signals of any current sensor will be filtered, conditioned and converted to baseband.

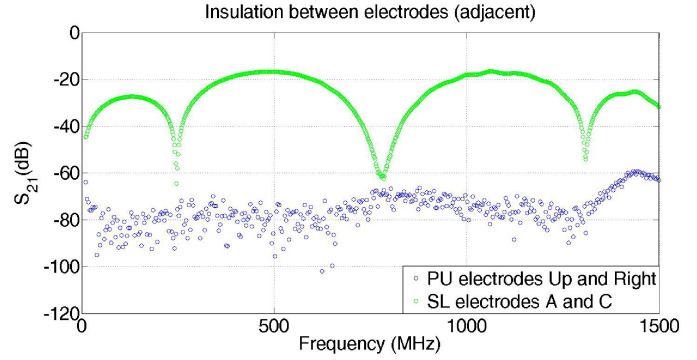


Figure 5: Detectors assembly for PU and SL.

- A DFE unit where the baseband signals are sampled to calculate the beam position, amplitude and phase, using a programmable hardware.

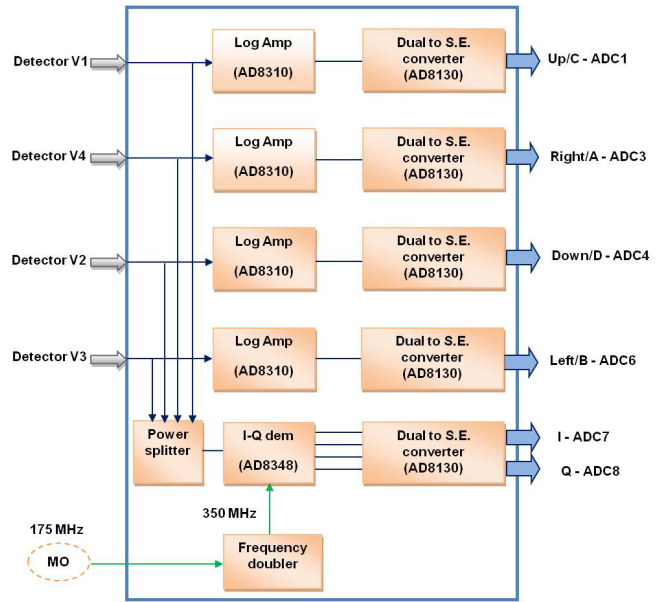


Figure 6: Schematic of the AFE unit of the BPM system.

3.1. Analog Front-End (AFE) unit

The AFE unit (Figs. 6 and 7) is responsible of filtering, conditioning and converting signals to base-band separating the information of the position, the amplitude and the phase of the beam [13], [16]. The AFE needs five input signals to operate correctly. Four are coming from the detectors of the test bench and the fifth one is the reference signal for the local oscillator (necessary for calculating the relative phase and the amplitude).

The method used to convert RF signals into baseband is based on the ESSB Low Level RF (LLRF) system [17], due to its easy and versatile implementation. This solution includes two in-house boards, a logarithmic amplifier (log amp) for measuring the position of the beam and an IQ demodulator for measuring the amplitude and the phase. To measure the X and Y beam positions, a 4-channel log amp board has been developed.

243 Each channel, based on the fast and high dynamic range AD8310
 244 log amp (95 dB), is connected to one of the four BPM sensors.
 245 The AD8310 log amp has 50 Ω impedance input. This module
 246 has a bandwidth large enough (around 500 MHz) allowing to
 247 measure a large variety of particle beams.

248 Figure 8 shows the characteristics of the logarithmic amplifier board.
 249 The upper graphic represents the dynamic range of one log amp channel.
 250 The graphic located below depicts the crosstalk measured injecting an input signal in channel one
 251 and the corresponding induced level in the different neighbour
 252 channels.

253
 254 The IQ demodulator is fed by the sum of the four BPM
 255 electrode signals. Each signal is converted from differential to
 256 single-ended using the AD8130 converter and sent to the DFE
 257 unit.

258 3.2. Digital Front-End (DFE) unit

259 The DFE unit consists of an FPGA (a high performance
 260 cPCI digital board based on a Xilinx [18] Virtex-4 with an additional
 261 14 bit ADC) connected to the control system. It calculates the beam
 262 position, amplitude and phase. This amplitude shows an estimation of
 263 the beam current. The programmable hardware based on an FPGA with
 264 the ADC boards (VHS-ADC board from Lyrtech company [19]) samples
 265 the baseband analog signals, with a high sample frequency of 105
 266 MHz, independently of the accelerated particle and its associated RF
 267 frequency.

268 Inside the FPGA, signals coming from the AFE are filtered to
 269 avoid noise and continuous components and the amplitude and phase
 270 of the beam are calculated using the CORDIC (Coordinate Rotation
 271 Digital Computer) algorithm [20]. As is explained in Section 4,
 272 detected signals are corrected to minimize the errors introduced by
 273 the AFE unit and the test bench. These will include the offset
 274 compensation and gain adjustment. As a result, using these corrected
 275 signals, the digital board provides the position, the amplitude and
 276 the phase of the beam with a high resolution.
 277
 278

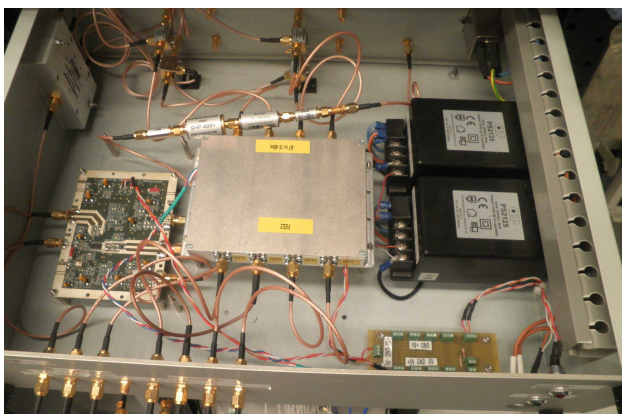


Figure 7: AFE unit including log amp and IQ demodulator boards, RF components and power supply distribution.

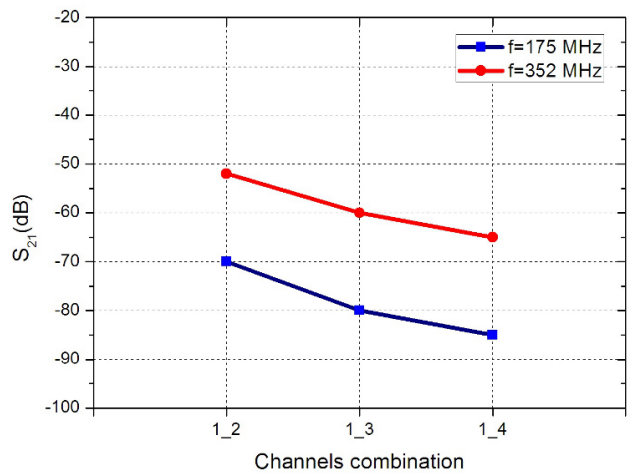
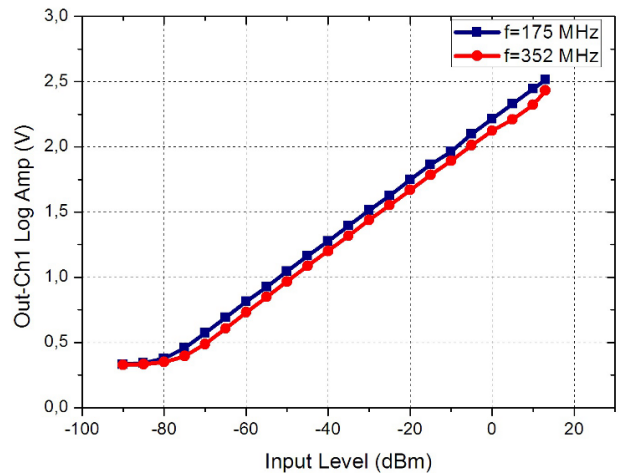


Figure 8: Measurements of the log amp board. Up: dynamic range of channel one. Down: crosstalk between the 4 channels of the same board.

279 3.3. BPM Control System

280 The fully integration of the BPM into an accelerator needs
 281 monitorization and archiving of the data. To handle these issues
 282 a Multipurpose Controller (MC) has been developed at ESS Bilbao [21], [22].
 283 Concretely, it gathers some tools to easily adapt the controller to any
 284 application.

285 The main elements of the MC are the Control Hardware, specific for
 286 each application (it can be any instrument or card like an FPGA based
 287 board, an oscilloscope,...), and the Head System computer, which
 288 performs the data acquisition, monitoring and storage [23], as well as
 289 the system configuration and the setup of the EPICS interface.

290 As is schematized in Fig. 9, the process to be monitored/controlled
 291 is connected to the Control Hardware, which establishes a communication
 292 channel with the Head System. Considering a generic application, the
 293 Control Hardware is dedicated to the acquisition and processing of the
 294 data and the generation of as many control signals as required. Then,
 295 the processed data is read by the Head System which controls the
 296 communication with the board and performs any further data processing.

297 Nevertheless, the Head System is not only responsible of

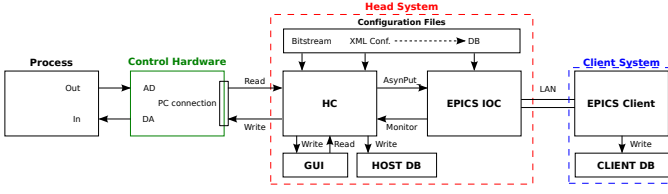


Figure 9: MC diagram.

the control hardware handling, but it also takes care of the EPICS server implementation and management, as well as the redundant local control. The Head System application structure can be split into two main blocks and an optional one: the Hardware Controller (HC) to manage the Control Hardware and the EPICS server to redirect the data to the Network.

One of the most important characteristics of the MC is its reconfigurability. It includes a single XML file, which contains all the information required of all the devices to be controlled. Once the user provides the file to the control software, it is parsed and used to successfully create any other configuration file which might be needed, like the EPICS database or any useful parameter.

Regarding the data logging capacity of the MC, two different ways of acting can be identified. On the one hand, there are the EPICS data logging clients which can be implemented fulfilling the users needs. On the other hand, the local data recording, directly from the HC into a MySQL database.

In the case of the BPM, the Control Hardware is implemented using a Lyrtech FPGA board and the Head System is implemented using a PC. Then, using the tools of the MC, the EPICS and Archiving integration is straightforward and reconfigurable by means of an XML file. In particular, this XML file includes the FPGA registers which acquire the data of the position monitors detectors, the set of signals to be included into the EPICS network and the calibration parameters. Hence, for example, this file is very useful when calibrating (next section) the BPM because the sensitivity parameters can be easily changed in the XML file by the operator. All the tools are easily accessed through the BPM control GUI, which is shown in Fig. 10.

4. Calibration and sensitivity of the BPM system

The calibration procedure is critical to calculate the correct position and to minimize errors. Two main calibrations can be performed in the system: the test bench calibration and the electronic calibration. Both of them are necessary to be able to translate the steps measured by the ADCs from the FPGA to real position values in mm.

4.1. Electronics calibration

The four signals coming from the test bench go inside the AFE unit, and then, to the ADC modules of the FPGA. The output of the FPGA is communicated with the control system, which is running on it. The calibration of the electronics allows to calculate the conversion equations to transform the steps

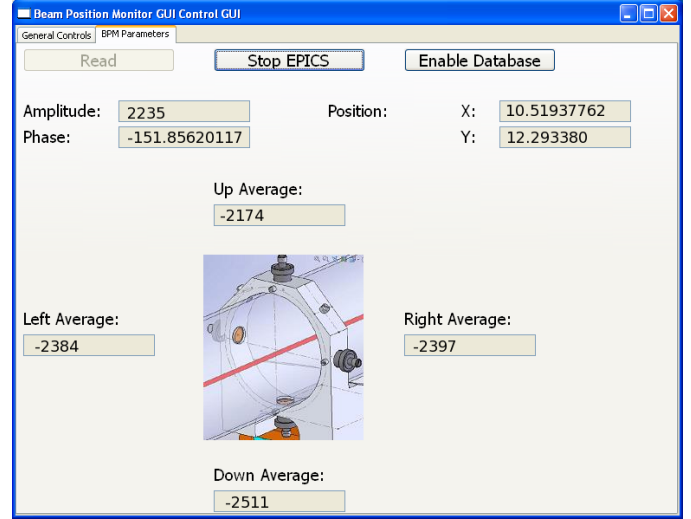


Figure 10: BPM Monitor GUI.

measured in the ADC channels of the DFE unit to the associated voltage values measured by the source detector. Knowing the detectors signal, it is possible to apply the $\frac{\Delta}{\Sigma}$ algorithm to interpret the signals from the four sensors accurately.

The $\frac{\Delta}{\Sigma}$ algorithm has been implemented in the HC, where the electrical center-of-mass beam position could be given by different expressions. Due to the assembly of both BPM detectors, two $\frac{\Delta}{\Sigma}$ algorithms have been used. The expressions selected for the PU BPM measurements have been the following:

$$X = \frac{\Delta_x}{\Sigma'} = \frac{U_{right} - U_{left}}{U_{right} + U_{left}} \quad (1)$$

$$Y = \frac{\Delta_y}{\Sigma''} = \frac{U_{up} - U_{down}}{U_{up} + U_{down}} \quad (2)$$

Other way to calculate the $\frac{\Delta}{\Sigma}$ algorithm is shown in the next equations used for stripline BPM calculations:

$$X = \frac{\Delta_x}{\Sigma} = \frac{(U_a + U_d) - (U_b + U_c)}{U_a + U_b + U_c + U_d} \quad (3)$$

$$Y = \frac{\Delta_y}{\Sigma} = \frac{(U_a + U_c) - (U_b + U_d)}{U_a + U_b + U_c + U_d} \quad (4)$$

where U_{right} , U_{left} , U_{up} , U_{down} , U_a , U_b , U_c and U_d are the voltages measured at each electrode of both BPM configurations. The electrical beam position is related to the real position through the inverse of the PU/SL sensitivities (see Equations (7), (8)).

4.2. Test bench calibration

After calculating the electrical beam position, the physical beam position is derived applying the test bench calibration parameters. To that end, the linearity of our test bench was characterized. Fig. 11 shows the differences between the real position and the obtained ones after the $\frac{\Delta}{\Sigma}$ algorithm. As it was expected, the BPM is more linear in the central area (the area

367 where the points are inside the rectangle). It is shown the non-378
 368 linear behaviour of the test bench, and also the relation of the 379
 369 nonlinearity with the distance to the center. Due to the non-380
 370 perfect linearity of the system an additional block had to be ad-381
 371 ded to the FPGA program for its linearization, the so-called test 382
 372 bench calibration block which is described next.

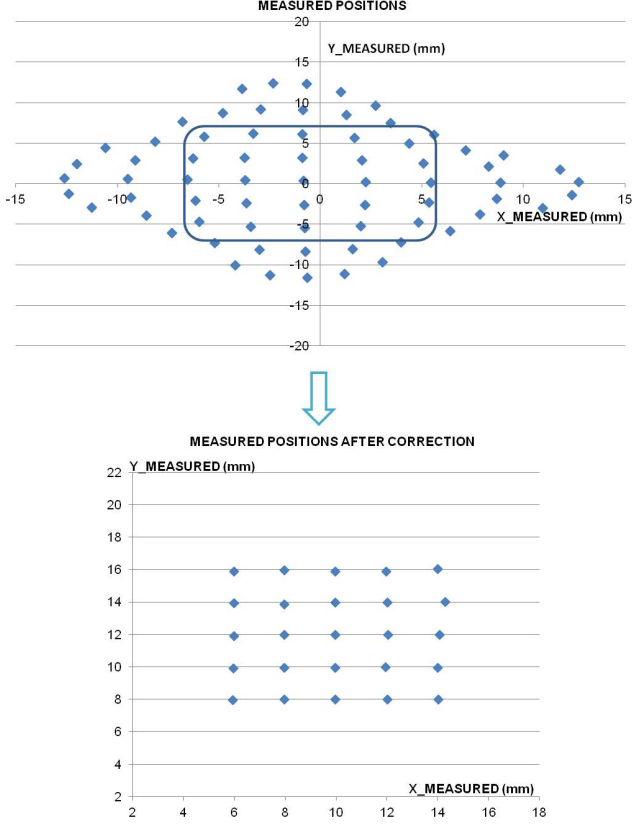


Figure 11: Linearization of the BPM test bench.

373 One possible solution for linearizing the system is presented
 374 in Equations (5), (6).

$$x_{real} = \sum_{i,j} a_{ij} \cdot X_{measured}^i \cdot Y_{measured}^j \quad (5)$$

$$y_{real} = \sum_{i,j} b_{ij} \cdot X_{measured}^i \cdot Y_{measured}^j \quad (6)$$

375 The coefficients a_{ij} and b_{ij} of the map functions that fit the
 376 measured position data were calculated. The order of the equa- 401
 377 tion was increased up to four to obtain a good fitting (Table 2).

Table 2: Results of the linearization fitting, showing the sum of squares due to 403
 error (SSE) and R-square

	SSE	R-square
$X_{linearization}$	3.28e-028	1
$Y_{linearization}$	9.46e-024	1

After calculating the coefficients and adding the lineariz-
 ation block corresponding to the test bench calibration, a new
 test was done to prove that the output of the BPM was improved
 (Fig. 11).

Taking into account that the linearization is based on previ-
 ous calibrations, it could be very sensitive to variations in the
 environment. Thus, a shielded electronics was used to main-
 tain the fitting goodness. The linearization was applied to the
 central area after calculating the electrical center, being the lin-
 earization results fully satisfactory.

4.3. Sensitivity of both BPMs

Although the previously presented linearization method is
 accurate, a trade off between complexity and accuracy has been
 adopted in real FPGA implementation. So, a first order polyno-
 mial function has been used as follows:

$$x = F_x(X, Y) = k_x \cdot X + \delta_x \quad (7)$$

$$y = F_y(X, Y) = k_y \cdot Y + \delta_y \quad (8)$$

393 The constants k_x and k_y are characteristics of the test bench
 394 and they are related with the sensitivities $S_{x,y}$ of the used moni-
 395 tors. $\delta_{x,y}$ represent the deviation of the beam from the center
 396 position.

$$k_{x,y} = \frac{1}{S_{x,y}(0,0)} \quad (9)$$

397 Table 3 shows the different sensitivities among the used de-
 398 tectors and working frequencies. The obtained sensitivity val-
 399 ues for PU are $S_{x,y} \approx 0.12 \text{ mm}^{-1}$ ($k_{x,y} \approx 8 \text{ mm}$) and for SL
 400 $S_{x,y} \approx 0.07 \text{ mm}^{-1}$ ($k_{x,y} \approx 13 \text{ mm}$).

Table 3: Test Bench Sensitivities for PU and SL at 352 and 175 MHz.

Pick-Up				
f (MHz)	$S_x[\text{mm}^{-1}]$	$S_y[\text{mm}^{-1}]$	δ_x	δ_y
352	0.1229	0.1182	10.37	11.96
175	0.1248	0.1252	10.32	12.06
Stripline				
f (MHz)	$S_x[\text{mm}^{-1}]$	$S_y[\text{mm}^{-1}]$	δ_x	δ_y
352	0.0717	0.0703	11.96	11.25
175	0.0791	0.075	12.36	11.81

5. Performance tests

In this section, the validation measurements for both BPM
 designs are described. The BPM system has been tested using
 the test bench, with both types of detectors, electronic units and
 the control system. Both detectors have been assembled and
 checked, PU first [13] and SL later [24], allowing the perform-
 ance comparison between both BPMs.

5.1. Experimental setup

Two different beams have been reproduced using RF equipment at 175 and 352 MHz:

- Sinusoidal signal in continuous wave mode.
- Sinusoidal signal in pulsed wave mode.

Connection diagrams used for continuous and pulsed wave measurements are slightly different. The generators are used to simulate the beam (in continuous and pulsed mode) and to generate the local oscillator signal needed for the AFE unit.

5.2. Resolution and stability

The detectable change in the developed system (position resolution) was measured calculating the standard deviation of the position data acquired at the center position capturing 10000 position values sampled at 105 MHz. The position of the beam is calculated using the log amp board. Its dependence on the input signal power is shown in Fig. 12, which shows the relation between the input signal level in the electronics and the resultant position resolution values. For both deployments, PU and SL, the resolution obtained for an input power signal in the logarithmic boards over -60 dBm is better than 10 μm .

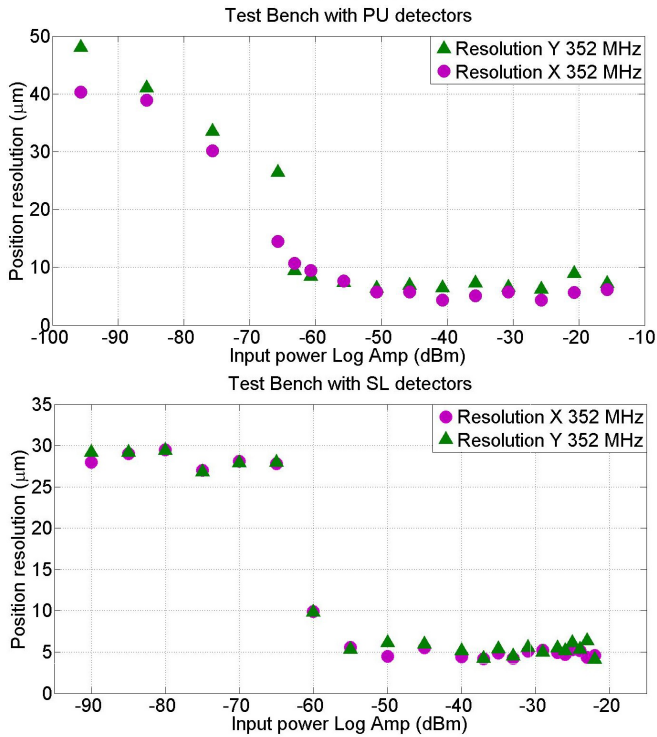


Figure 12: Position resolution at different input powers for PU (up) and SL (down) BPMs.

Tables 4-7 show the results for a given input beam power signal. The long term stability is affected by drifts in the electronics due to temperature variations. The temperature has been monitored for several months and variations of less than 10 °C have been measured. Under these conditions, the system stability values have been maintained under the required specifications shown in Table 1. The long term stability has been calculated in the same way as the resolution but during a bigger

time period. In addition, the resolution and the stability are also affected by vibrations, noise, cabling effects, etc.

The power levels used in continuous and pulsed wave mode are similar. The input levels of the generators have been configured to have always a similar signal level at the input of the electronics. In this way, the average input signal seen by the electronics should be similar in both cases. Tables 4-7 show the obtained results for a fixed input signal power (detectable by the AFE unit). The signal level, locating the simulated beam in the center of the tube, is -25 dBm detected by the log amp board and is -30 dBm measured by the IQ demodulator board.

Table 4: PU BPM results in continuous wave mode

Parameter	175 MHz	352 MHz	Unit
X axis Resolution (rms)	4	4.28	μm
Y axis Resolution (rms)	4.74	6.46	μm
Phase Resolution (rms)	0.11	0.116	$^\circ$
X axis Stability (rms)	5.24	7.74	μm
Y axis Stability (rms)	21.36	26.7	μm
Phase Stability (rms)	0.204	0.386	$^\circ$

Table 5: PU BPM results in pulsed wave mode

Parameter	175 MHz	352 MHz	Unit
X axis Resolution (rms)	5.8	3.8	μm
Y axis Resolution (rms)	6.03	5.5	μm
Phase Resolution (rms)	0.11	0.095	$^\circ$
X axis Stability (rms)	8.32	7	μm
Y axis Stability (rms)	33.1	36.8	μm
Phase Stability (rms)	0.828	1.317	$^\circ$

Table 6: SL BPM results in continuous wave mode

Parameter	175 MHz	352 MHz	Unit
X axis Resolution (rms)	5.71	5.37	μm
Y axis Resolution (rms)	5.83	5.19	μm
Phase Resolution (rms)	0.07	0.1	$^\circ$
X axis Stability (rms)	12.06	9.59	μm
Y axis Stability (rms)	14.47	15.66	μm
Phase Stability (rms)	0.14	0.09	$^\circ$

Table 7: SL BPM results in pulsed wave mode

Parameter	175 MHz	352 MHz	Unit
X axis Resolution (rms)	5.37	5	μm
Y axis Resolution (rms)	5.29	6.03	μm
Phase Resolution (rms)	0.01	0.05	$^\circ$
X axis Stability (rms)	17.13	19.02	μm
Y axis Stability (rms)	22.71	15.2	μm
Phase Stability (rms)	2.54	2.52	$^\circ$

All the results are fulfilling the requirements in Table 1.

With all the BPM system assembled, the obtained position and phase resolution values are very similar for the different configurations.

In general, the results for a continuous simulated beam are slightly more accurate with respect to the results for pulsed simulated beam. This minimal difference is affected by the implementation philosophy selected for pulsed mode (a single sample has been measured every pulse) and also because of the response time of the electronic units.

The presented slight differences, which do not compromise the ESSB Linac requirements, are due to the test bench assembling imperfections and environmental variations between measurements. From these results, it can be deduced that both PU and SL are within specifications, both for continuous and pulsed regimes.

The phase measurements shown before are relative to the RF main frequency. To prove that the phase is well calculated, phase variations have also been measured, introducing known delays in the cabling, always obtaining the expected value to less than 1° error.

6. Summary and Conclusions

A new versatile electronics system for the ESSB beam position monitors has been presented. The proposed design has been conceived to be fully configurable so that it could eventually be used in different kind of proton or ion accelerators with minimal change.

The system includes both button-type pickups or striplines as detectors and an analog front-end plus a digital unit, with a control system which integrates EPICS and Archiver. Both type of detectors, button-type pickups and striplines are complementary. Button-type detectors are the simplest monitors which present better mechanical properties and a smoother power response in a broader frequency band. Nevertheless, for low beam currents, button-type detectors signal level is weaker than striplines response, which have a significantly better response for low beam currents and could be used for very low frequencies. Several tests have been performed at simulated proton and deuteron beamlines at 352 MHz and 175 MHz RF frequencies, leading to resolution and accuracy values fulfilling ESSB requirements. As a whole, the presented BPM system, composed of the BPM electrode block, the analog and digital electronic units and the control system, constitutes an all-in-one integrated and serializable solution for accurate beam position and phase monitoring in ion accelerators.

Finally, next steps towards industrialization of the presented BPM system need to assure the robustness of the solution in a real particle accelerator environment. To this end, on the one hand, the BPM mechanical blocks will be manufactured using high-vacuum-compatible parts, ready to be integrated in the real beamline. On the other hand, the electronics and proposed acquisition solution will be translated to the PCI eXtensions for Instrumentation (PXI) architecture, to benefit from a solid, dominant and extended open industry standard, ensuring upgradeability and easy maintenance of the Digital Front-End Unit as well as automation of the calibration process.

References

- [1] P. Strehl, *Beam Instrumentation and Diagnostics*, Springer, 2006.
- [2] R.E. Shafer, Beam position monitoring, in: AIP conference proceeding 212, Upton, NY, 1989, pp. 26–58.
- [3] G. Vismara, The comparison of signal processing systems for beam position monitors, in: Proceedings of DIPAC'99, IT05, Chester, UK, 1999, pp. 12–18.
- [4] T. Suwada, N. Kamikubota, H. Fukuma, N. Akasaka, H. Kobayashi, Stripline-type beam-position-monitor system for single-bunch electron/positron beams, *Nuclear Instruments and Methods in Physics Research Section A* 440 (2) (2000) 307–319.
- [5] M. Cohen-Solal, Design, test, and calibration of an electrostatic beam position monitor, *Phys. Rev. ST Accelerators and Beams* 13, 032801 (2010) 1–13.
- [6] Log-ratio BPM electronics (2013).
URL http://www.bergoz.com/index.php?option=com_content&view=article&id=31&Itemid=40
- [7] Instrumentation technologies (2013).
URL <http://www.i-tech.si/accelerators-instrumentation>
- [8] P. Hartmann, J. Fursch, D. Schirmer, T. Weis, K. Wille, Experience with libera beam position monitors at DELTA, in: Proceedings of DIPAC2007, TUPB21, Venice, Italy, 2007, pp. 111–113.
- [9] F.D. Wells, J.D. Gilpatrick, R.E. Shafer, R.B. Shurter, Logratio circuit for beam position monitoring, 14th IEEE Particle Accelerator Conference, San Francisco, CA, USA (1991) 1139–1141.
- [10] R.B. Shurter, Analog front-end electronics for beam position measurement on the beam halo measurement, 2001 Particle Accelerator Conference, Chicago 2 (2001) 1378–1380.
- [11] S. Walston, S. Boogert, C. Chung, P. Fitsos, J. Frisch, J. Gronberg, H. Hayano, Y. Honda, Y. Kolomensky, A. Lyapin, S. Malton, J. May, D. McCormick, R. Meller, D. Miller, T. Orimoto, M. Ross, M. Slater, S. Smith, T. Smith, N. Terunuma, M. Thomson, J. Urakawa, V. Vogel, D. Ward, G. White, Performance of a High Resolution Cavity Beam Position monitor system, *Nuclear Instruments and Methods in Physics Research A* 578 (2007) 1–22.
- [12] E. Abad, I. Arredondo, I. Badillo, D. Belver, F.J. Bermejo, I. Bustinduy, D. Cano, D. Cortazar, D. de Cos, S. Djekic, S. Domingo, P. Echevarria, M. Eguiraun, V. Etxebarria, D. Fernandez, F.J. Fernandez, J. Feuchtwanger, N. Garmendia, G. Harper, H. Hassanzadegan, J. Jugo, F. Legarda, M. Magan, R. Martinez, A. Megia, L. Muguira, G. Mujika, J.L. Muoz, A. Ortega, J. Ortega, M. Perlado, J. Portilla, I. Rueda, F. Sordo, V. Toyos, A. Vizcaino, ESS-Bilbao light-ion linear accelerator and neutron source: design and applications, *Journal of Physics: Conference Series* 325 012003 (1) (2011) 1–6.
- [13] D. Belver, I. Arredondo, M. Del Campo, P. Echevarria, J. Feuchtwanger, N. Garmendia, H. Hassanzadegan, L. Muguira, F.J. Bermejo, V. Etxebarria, J. Jugo, J. Portilla, Overview of the BPM system of the ESS-Bilbao, in: Proceedings of DIPAC2011, MOPD21, Hamburg, Germany, 2011.
- [14] K. Iwamoto, Y. Ikeda, T. Kitamura, T. Matsuoka, Design of cold BPM feedthrough, in: Proceedings of EPAC2008, TUPC041, Genoa, Italy, 2008.
- [15] S. Varnasseri, I. Arredondo, D. Belver, F.J. Bermejo, J. Feuchtwanger, N. Garmendia, P.J. Gonzalez, L. Muguira, V. Etxebarria, J. Jugo, J. Portilla, Design and fabrication of the stripline BPM at ESS-Bilbao, in: Proceedings of IBIC2012, MOPA31, Tsukuba, Japan, 2012.
- [16] D. Belver, I. Arredondo, M. Del Campo, P. Echevarria, J. Feuchtwanger, N. Garmendia, H. Hassanzadegan, L. Muguira, F.J. Bermejo, V. Etxebarria, J. Jugo, J. Portilla, J.M. Carmona, A. Guirao, A. Ibarra, L. M. Martinez Fresno, I. Podadera, Test of the front-end electronics and acquisition system for the lipac BPMs, in: Proceedings of IPAC2011, TUPC125, San Sebastian, Spain, 2011.
- [17] H. Hassanzadegan, N. Garmendia, V. Etxebarria, F. J. Bermejo, Low level RF system for the european spallation sources bilbao linac, *Physical Review ST Accelerators and Beams* 14 052803 (5) (2011) 1–16.
- [18] All programmable technologies from xilinx inc. (2013).
URL <http://www.xilinx.com/>
- [19] Nutaq - DSP & FPGA solutions supplier - experts in digital signal processing (2012).
URL <http://nutaq.com/en/>

- 573 [20] J.E. Volder, The CORDIC trigonometric computing technique, IRE
574 Transactions on Electronic Computers EC-8 (3) (1959) 330–334.
- 575 [21] I. Arredondo, M. Del Campo, P. Echevarria, D. Belver, L. Muguira, N.
576 Garmendia, H. Hassanzadegan, V. Etxebarria, J. Jugo, Fast acquisition
577 multipurpose controller with EPICS integration and data logging, in: Pro-
578 ceedings of IPAC2011, WEPC155, San Sebastian, Spain, 2011.
- 579 [22] I. Arredondo, M. Del Campo, P. Echevarria, J. Jugo, V. Etxebarria, Mul-
580 tipurpose controller with EPICS integration and data logging: BPM ap-
581 plication for ESS bilbao, Nuclear Instruments and Methods in Physics
582 Research Section A: Accelerators, Spectrometers, Detectors and Associ-
583 ated Equipment. Submitted. 2013.
- 584 [23] EPICS (Jul. 2011).
585 URL <http://www.aps.anl.gov/epics>
- 586 [24] D. Belver, F.J. Bermejo, J. Feuchtwanger, N. Garmendia, P.J. Gonza-
587 lez, L. Muguira, S. Varnasseri, V. Etxebarria, J. Jugo, J. Portilla, Design
588 and measurements of the stripline BPM system of the ESS-Bilbao, in:
589 Proceedings of the 3rd International Particle Accelerator Conference
590 IPAC2012, MOPPR041, New Orleans, Louisiana, 2012.